

Development of gear fault diagnosis architecture for combat aircraft engine

Rajdeep De and S.K. Panigrahi*

Department of Mechanical Engineering, DIAT (DU), Girinagar, Pune, Maharashtra, 411025, India

(Received August 4, 2022, Revised May 2, 2023, Accepted July 31, 2023)

Abstract. The gear drive of a combat aircraft engine is responsible for power transmission to the different accessories necessary for the engine's operation. Incorrect power transmission can occur due to the presence of failure modes in the gears like bending fatigue, pitting, adhesive wear, scuffing, abrasive wear and polished wear etc. Fault diagnosis of the gear drive is necessary to get an early indication of failure of the gears. The present research is to develop an algorithm using different vibration signal processing techniques on industrial vibration acquisition systems to establish gear fault diagnosis architecture. The signal processing techniques have been used to extract various feature vectors in the development of the fault diagnosis architecture. An open-source dataset of other gear fault conditions is used to validate the developed architecture. The results is a basis for development of artificial intelligence based expert systems for gear fault diagnosis of a combat aircraft engine.

Keywords: combat aircraft; diagnosis architecture; failure modes; gears; signal processing techniques

1. Introduction

In modern combat aircraft engines, the accessory units are driven by a gear drive system consisting of the internal gearbox, radial main shaft, direct drive/gear train drive, intermediate gearbox, external gearbox and auxiliary gearbox. Different types of gearbox designs are used for driving the accessory units. The most common type of aircraft engine gearbox is a planetary gearbox. The radial main shaft induces more thermal fatigue and flow disturbances in the turbine region. So, the internal gearbox is generally mounted within the compressor region. The spool of the high-pressure region is rotated to produce airflow in the engine. As a result, the internal gearbox, which is coupled to the compressor shaft of the high-pressure section, is subjected to rotary motion. Generally, bevel gears are used for meshing. The radial main shaft is used for power transmission from the internal gearbox to both the accessory unit and the external gearbox. It is placed within the compressor support structure and has a small diameter. The diameter should not be too small to stop the airflow disruption. Otherwise, it can lead to vibrations in the gearbox. Sometimes because of space constraints, an intermediate gearbox is used for power transmission from the radial main shaft to the external gearbox. Generally, bevel gears are used for meshing. The external gearbox is used for power transmission to the engine's different accessory units and used as a mounting surface for each accessory unit (www.academia.edu). Sometimes a direct drive

*Corresponding author, Professor, E-mail: panigrahi.sk@gmail.com

or a gear train drive can be used to transmit power to accessory units located at a long distance from the external gearbox. Generally, spur and helical gears are used for meshing. However, helical gears can sometimes give rise to end thrust, so spur gears are used primarily. As all the accessory units cannot be mounted on the external gearbox, sometimes an auxiliary gearbox is used to transmit power to the additional accessory units. The auxiliary gearbox functions similarly to an external gearbox.

The performance of the gear drive of an aircraft engine directly influences the efficiency of the engine's other components. The presence of faults in the gears adversely affects the performance of the gear drive. Since an aircraft engine performs many functions during its operation, defects can occur in gears during any function and, if left undetected, can lead to significant engine failures. Hence there is a need for efficient fault diagnosis systems that can give indications about the possible failure of the gear drive (www.machinerylubrication.com).

Gears are subjected to different failure modes (Prabhu R and Devaraju A, 2021), and one may need to identify the exact modes of failure such as fatigue (Čular *et al.* 2023, Chen *et al.* 2021), tooth wear (Huang fu *et al.* 2020), and vibrations (Luo *et al.* 2021, Sunder and Hemalatha 2021) etc. Gears subjected to repeated loading can undergo bending fatigue. In bending fatigue, microscopic cracks are developed in stress concentration regions of discontinuities. These cracks slowly progress to cause sudden fracture. The tooth root fillet is the primary point of occurrence of gear tooth failures. The broken tooth pieces caused by bending fatigue can cause damage to the other gearbox components, such as the shaft and bearings. Cyclic contact stresses can cause surface fatigue. The most common type of this fatigue phenomenon is pitting. Errors in tooth profile, surface irregularities and misalignment can contribute to the formation of localized pits. Sometimes these pits can cause progressive damage to the tooth surface. The dedendum region between the tooth root and the pitch line is the most common point of occurrence of pitting. The presence of different mechanical, chemical and electrical forces acting on the face of the gear tooth can lead to wear of the gear tooth surface. Wear can be classified into three major types-adhesion, abrasive and polished. Adhesion is mainly caused by the interaction of oxide layers of two gear teeth. Sometimes it can lead to excessive wear on the tooth surface. Scuffing is severe adhesion which causes metal transfer between two surfaces. Sometimes, plastic deformation and tooth tip displacement take place. Contaminants in lubricants can cause abrasion so that the tooth thickness is reduced significantly. Polishing causes fine scratches on the surface due to impurities present in the lubricants. The ends of the contact area and the dedendum are affected heavily due to severe polishing.

For online fault diagnosis of the gear drive of a combat aircraft engine, vibration data is acquired using the data acquisition systems for long flight durations and different flight stages. MATLAB based systems have limitations in dealing with complex vibration data using direct algorithms for gear fault diagnosis. The developed architecture is compatible with the data acquisition systems of a combat aircraft engine and hence can be used as a suitable alternative for gear fault diagnosis. The developed architecture applies advanced signal processing techniques on the raw vibration signals from the accelerometers to take into account the geometric nonlinearity. The developed architecture is tested with own code in MATLAB to determine the efficiency with which it can detect the presence of gear faults directly from the raw vibration signals without the need of any manual processing. The appropriate feature vector for each fault is then determined so that the resultant dataset can be used with machine learning algorithms to further develop expert-based systems to identify the exact type of fault from the gear vibration signals.

In Section 2, a literature review of different signal processing techniques is discussed. Section 3 discusses the characteristics of gear vibration and the different types of vibration signals that will

be required to extract the different feature vectors. The mathematical expressions of the different feature vectors are also stated that will be used for development of the architecture. Section 4 explains the detailed process for the development of the architecture and validation of the architecture using an open-source dataset. Section 5 compares the results from the developed architecture with the results obtained from own code in MATLAB.

2. Fault diagnosis techniques used for combat aircraft gearbox

Time-domain signal processing methods have been extensively adopted for fault diagnosis of gearboxes due to easy and direct approach compared to other methods. A technique has been presented to calculate the averages in the time domain for tooth meshing of planet gears and sun gear (McFadden 1991). The technique has been validated with vibration data from a planetary gearbox test rig with seeded damage (McFadden and Howard 1990). The effect on condition indicators such as root mean square and standard deviation has been studied to distinguish between a helicopter gearbox's cracked and healthy carrier gear (Wu *et al.* 2005). The influence of external varying loading conditions on the vibration characteristics of a developed gearbox system has been studied (Bartelmus and Zimroz 2009), and a new diagnostic feature has been designed for monitoring gearbox failure in non-stationary conditions (Bartelmus and Zimroz 2009). An attempt has been made to collect vibration data by mounting transducers internally on the rotating gear and applying the synchronous averaging technique for fault diagnosis of planetary gearboxes (Smidt, 2010). Health indicators have been extracted for fault diagnosis of gearboxes used in oil sands operations using the time-synchronous averaging technique to preprocess vibration data (Yip 2011). Modifications have been done in several traditional diagnostic parameters, such as FM0 and FM4, for planetary gearbox applications (Keller and Grabill, 2003). From the analysis, only two parameters have been performed relatively well for lab test conditions, but none are adequate for on-aircraft conditions (Keller and Grabill 2003).

Researchers have applied frequency-domain signal processing methods to overcome the limitations of time-domain methods. A simple frequency-domain method has been suggested to eliminate the changes in vibration amplitudes due to the effects of transducers and structural path for the implementation of early fault detection of a planetary ring gear (Mark *et al.* 2010). The fault characteristic frequencies of each component of a planetary gearbox used in underground coal mining have been examined for the diagnosis of gear damage (Singleton 2006). Using Fast Fourier Transform, index vectors have been designed for distinguishing the healthy and faulty carrier gear of a helicopter planetary gearbox (Sparis and Vachtsevanos 2022). A lot of computational methods are available to diagnose gear damages. Recently, the damped vibration is performed (Heydari 2021) for the annular and rectangular graded beams in the presence of the attached lumped mass. A frequency-domain feature named energy ratio has been developed by applying time-synchronous averaging on a preprocessed signal to determine a crack in a planetary carrier (Hines *et al.* 2005). Fourier series has been applied to process vibration data captured from a helicopter planetary gearbox and a possible explanation for the asymmetry phenomena observed in the spectra has been deduced (McNames 2001).

Researchers have applied time-frequency-domain signal processing methods to diagnose planetary gearboxes because of their better effectiveness. Wigner-Ville distribution has been used to analyze signals simulated with tooth pitting and crack for fault diagnosis of planetary gearboxes (Chaari *et al.* 2006). An adaptive filtering technique in conjunction with time-frequency methods

has been proposed for the health monitoring of a planetary gearbox (Schön 2005). Local mean decomposition has been used to diagnose a seeded crack fault in a wind turbine (Liu *et al.* 2012). A joint amplitude and frequency demodulation method has been proposed to diagnose sun gear damage of a gearbox test rig using ensemble empirical mode decomposition and energy separation algorithm (Feng *et al.* 2012). The use of complex Morlet wavelets for extraction of features for faulty and healthy carrier gear has been employed for a helicopter gearbox (Saxena *et al.* 2005). The auto covariance of maximal energy wavelet coefficients has been analyzed to study the advancement of faults in a gearbox used for oil sand operations (Yu 2011). A denoising method based on adaptive Morlet wavelets and singular value decomposition have been applied to extract impulse features of a wind turbine gearbox (Jiang *et al.* 2011).

Although the traditional signal processing methods are useful for gear fault diagnosis, the determination of faults requires some degree of expertise. Thus, various intelligent diagnosis methods have been studied by researchers so that expert systems can be developed for gear fault diagnosis. The use of Neural Networks to detect gear tooth wear and tooth breakage has been investigated (Sanz and Huerta 2012, Ma *et al.* 2005, Chen and Wang 2002, Cirrincione *et al.* 2020). Efforts have been made to develop model-based systems for diagnosing tooth crack (Wang and Makis 2009, Yang *et al.* 2019 and Liu *et al.* 2018). The use of a Support Vector Machine (SVM) to classify gear faults has been investigated (Bansal *et al.* 2013, Chen *et al.* 2016, Saravanan *et al.* 2010, Xing *et al.* 2017). For a more accurate diagnosis of fault and pitting in gears, self-organizing maps have also been used (Cheng *et al.* 2013, Jing *et al.* 2017, Qiang *et al.* 2020, Li *et al.* 2012).

Modern fault diagnosis systems using vibration signals are dependent on the extraction of suitable feature vectors. Different methods have been used for feature extraction from vibration signals using empirical wavelet transform (Li *et al.* 2021), reverse dispersion entropy and refined composite multi-scale dispersion entropy (Li *et al.* 2022).

The present study primarily develops a gear fault diagnosis architecture to analyze raw vibration data captured from combat aircraft engine accelerometers using signal processing techniques. An open-source dataset of different gear faults is analyzed on combat aircraft engine customized data analysis systems to extract the required feature vectors that indicate the presence of faults in the gear data. The results of the feature vectors are validated with the results from obtained by using own code in MATLAB. The results provide a theoretical basis for developing artificial intelligence-based expert systems for gear fault diagnosis.

3. Theoretical background

3.1 Gear vibration characteristics

It is impossible to manufacture perfect gears with desired tooth profiles, concentricity and meshing characteristics. Hence, it is very common for gear mesh vibration takes place in a gear assembly (www.cbmconnect.com). Gear mesh frequency is a characteristic of the frequency spectrum of a gear assembly and is given by the product of the number of gear teeth and the rotating speed of the gear (www.power-mi.com). For all gear conditions, gear mesh frequency corresponds to the maximum amplitude in the frequency spectrum of the gear. Gear mesh frequency sidebands are equidistant frequencies from the gear mesh frequency corresponding to the rotating frequency of the pinion and the gear (www.power-mi.com). If the vibration amplitude values become very high at the gear mesh frequency, it indicates a failure in the gears. Sometimes

due to wear on the gear surface, an increase in amplitude is noticed at the harmonics of the gear mesh frequency with very little change in amplitude at the fundamental gear mesh frequency. This is because tooth engagement can result in several impacts leading to excitation of the gear forces (www.cbmconnect.com). The position of the sidebands in the frequency spectrum also gives an idea about the location of defects in the gear assembly (www.cbmconnect.com). Suppose, for a two-gear assembly, if the defect is present on any one gear, the sidebands are spaced above and below the gear mesh frequency at a frequency equal to the rotating frequency of the defective gear. Again, if the defects are present on both the gears, then there are two families of sidebands in the frequency spectrum corresponding to each defective gear.

3.2 Types of gear vibration signals

The raw vibration signals acquired from accelerometers attached to the gearbox need to be processed to generate the required signals for vibration analysis using different algorithms. Time-synchronous averaged, residual, differential and regular signals are used for fault diagnosis. These are derived by applying various signal processing techniques on the raw signals.

Time synchronous averaging is a technique of averaging time-domain signals over uniform rotation angles or complete rotations such that noise and disturbances are gradually filtered out. This is done by using tachometer signals to determine the pulses per rotation. The time synchronous averaging technique helps filter out the disturbances and noise that is non-synchronous with the tachometer signal.

The residual signal is derived from the time-synchronous averaged signal by using band-stop filters to remove the harmonics of the shaft frequency and gear meshing frequency. The differential signal is derived from the residual signal by using band-stop filters to remove the first-order sidebands of the harmonics of the gear meshing frequency. The periodic signal is derived from the time-synchronous averaged signal by using band-pass filters to extract the harmonics of the shaft frequency and gear meshing frequency.

3.3 Description of the feature vectors

Using the vibration analysis techniques, the feature vectors are computed, giving an idea about the faults' appearance. These feature vectors are discussed in the following section:

- R.M.S. - It gives an idea about the signal dataset's vibration amplitude and energy content. This feature vector has been found to indicate general fault progression in gears (Decker 2002, Večeř *et al.* 2005, Bechhoefer *et al.* 2013, James and Wu *et al.* 2008).

$$S_{RMS} = \sqrt{\frac{1}{N} \sum_1^N (s_i)^2} \quad (1)$$

where S_{RMS} is the RMS value of the signal dataset s .

- Kurtosis- It gives an idea about the presence of peaks in the signal dataset. If the value is close to 3, it indicates a Gaussian distributed noise signal. This feature vector has been found to indicate breakage and wear in gears (Decker 2002, Bechhoefer *et al.* 2013, Wu *et al.* 2008, Wang 2001).

$$S_{Ku} = \frac{N \times \sum_1^N (s_i - \bar{s})^4}{\left\{ \sqrt{\sum_1^N (s_i - \bar{s})^2} \right\}^4} \quad (2)$$

where S_{KU} is the Kurtosis value of the signal dataset s .

- Crest Factor (CF) - It is used to detect faults in gears at an early stage. The CF of a sine wave is about 1.414. This feature vector has been found to indicate impulsive vibration due to tooth breaks in gears (Decker 2002, Bechhoefer *et al.* 2013).

$$S_{CF} = \frac{S_{peak}}{S_{RMS}}, \quad S_{peak} = \max(s_1, s_2, s_3, \dots, s_N) \quad (3)$$

where S_{peak} is the maximum value of the signal dataset s and

S_{CF} is the Crest Factor value of the signal dataset s .

- Energy Ratio (ER) - It is the ratio of the energy content of the differential signal and the energy content of the regular meshing component of the signal. This feature vector has been found to indicate heavy wear, i.e., damage on more than one tooth of a gear (Zhang *et al.* 2013).

$$S_{ER} = \frac{\sigma(d)}{\sigma(r)} \quad (4)$$

where S_{ER} is the Energy Ratio value of the signal dataset s ,

$\sigma(d)$ is the standard deviation of the differential signal and $\sigma(r)$ is the standard deviation of the regular signal.

- Fourth Order Figure of Merit (FM4) - It gives an idea about the presence of peaks in the differential signal of a gear. A value close to 3 indicates a signal of Gaussian distributed noise. This feature vector has been found to indicate wear/scuffing/pitting and tooth bending due to root cracks in gears (Decker 2002, James *et al.* 2000, Decker and Lewicki 2003 and Shen *et al.* 2011).

$$S_{FM4} = \frac{N \times \sum_1^N (d_i - \bar{d})^4}{\{\sum_1^N (d_i - \bar{d})^2\}^2} \quad (5)$$

where S_{FM4} is the FM4 value of the signal dataset s or Kurtosis value of the differential signal d .

- Sixth Order Differential Moment (M6A) and Eighth Order Differential Moment (M8A) - These are applied on a differential signal and are found to be more sensitive to peaks. These two feature vectors have been found to act as a surface damage indicator for gears (Decker 2002).

$$S_{M6A} = \frac{N^2 \times \sum_1^N (d_i - \bar{d})^6}{\{\sum_1^N (d_i - \bar{d})^2\}^3} \quad (6)$$

where S_{M6A} is the M6A value of the signal dataset s or M6 value of the differential signal d

$$S_{M8A} = \frac{N^2 \times \sum_1^N (d_i - \bar{d})^8}{\{\sum_1^N (d_i - \bar{d})^2\}^4} \quad (7)$$

where S_{M8A} is the M8A value of the signal dataset s or M8 value of the differential signal d .

- NA4- It is applied on a residual signal and uses the run-time averaged variance of the residual signal for calculations. This feature vector is used to detect progressive damage in gears (James and Limmer 2000, Zakrajsek *et al.* 1993, Zakrajsek and Lewicki 1996 and Dempsey and Zakrajsek 2001).

$$S_{NA4} = \frac{N \times \sum_1^N (r_i - \bar{r})^4}{\{1/M \times \sum_1^M \sum_1^N (r_{ij} - \bar{r})^2\}^2} \quad (8)$$

where S_{NA4} is the NA4 value of the signal dataset s or the fourth-order run-time averaged moment of the residual signal 'r'.

4. Methodology

4.1 Development of gear fault diagnosis architecture

Referring to Fig. 1, the flow chart of gear fault diagnosis architecture consisting of the time-domain vibration signal dataset for each condition is stored in a .CSV file having the same number of columns as the number of runs for the condition. Each CSV file is imported in the form of a 2D plot with time as the independent variable by defining the sampling rate in samples/sec and replacing the missing data with zeroes. The vibration signal dataset is synchronized with the tachometer signal dataset stored in the CSV file and imported in the form of a 2D plot with time as the independent variable. The resultant signal is averaged to remove the noise and disturbances from the signal. Considering each signal dataset to be in time-synchronous averaged form, residual, differential and regular signals are derived by using Chebyshev Band Filter. A Chebyshev filter has a much steeper cut-off rate than the corresponding Butterworth Filter at the cost of some ripples in the pass band. For removing a range of frequencies from the signal, band-stop filtering is done, and band-pass filtering is done for extracting a range of frequencies. The signal is filtered by specifying the upper and lower cut-off range of frequency. Generally, the range of lower cut-off frequency varies from 0.0 to half the sampling rate, and the range of higher cut-off frequency varies from lower cut-off frequency to half the sampling rate.

No filtering will occur if the lower limit of frequency is equal to 0.0 and the upper limit of frequency is equal to half the sampling rate. If phase less filtering is used, the data is passed through a filter of half the required cut-off rate twice, once forward and in reverse. The actual frequency response function differs slightly because two filters, each with $(N/2)$ poles, are used rather than one N pole filter. After computing the residual signal, differential signal and regular signal for each input signal dataset, the output signal dataset is read to a .CSV file so that it can be used in the subsequent steps. For calculating the root mean square and the crest factor of the input signal, parameters such as integration length, output interval step, interval-style and center of first integration need to be defined. The interval style can be set either as a number of points or in terms of the independent variable. The integration length defines the section of the signal for which the values are to be calculated. If the center of the first integration is not specified, the base of the output signal will be set to (Base of the input signal + half the integration duration). If the center of the first integration is specified, the base of the output signal will be set to (Centre of first integration- half the integration duration). The input signal is normalized to zero mean to calculate even order moments of the time-synchronous averaged signal and differential signal. The normalized signal is raised to the power of the same value as the order of the moment. The mean is calculated for the normalized signal raised to the required power. The mean is divided by the standard deviation of the input signal raised to the power of the same value as the order of the moment. The resultant value gives the required even order moments. For calculating the energy ratio parameter, the standard deviation of the differential signal is divided by the standard deviation of the regular signal. For calculating the NA4 parameter, the run-time averaged variance of the residual signal is evaluated. The run-time averaged variance is determined by calculating the ensemble power average of the variance for all signals preceding the signal of interest in the run ensemble. The square of the run-time averaged variance is used to divide the mean of the normalized residual signal raised to the fourth power. The resultant value gives the required NA4 parameter.

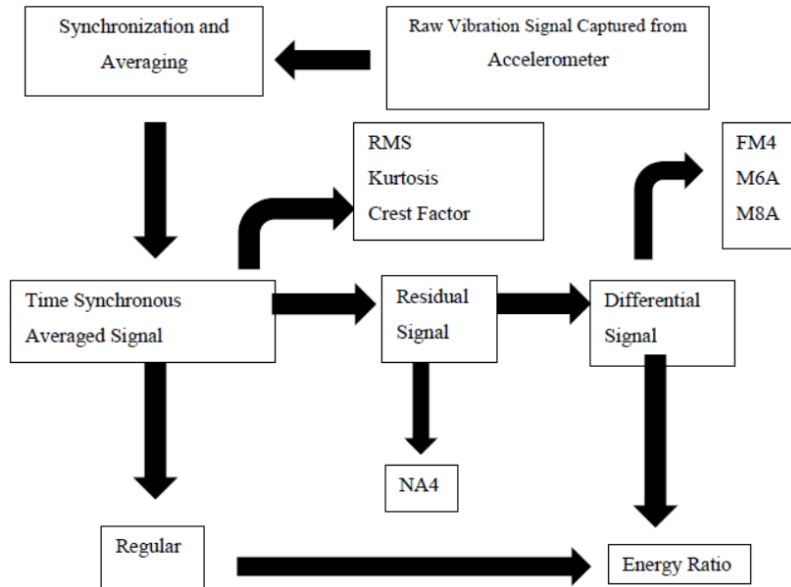


Fig. 1 Flow chart of gear fault diagnosis architecture

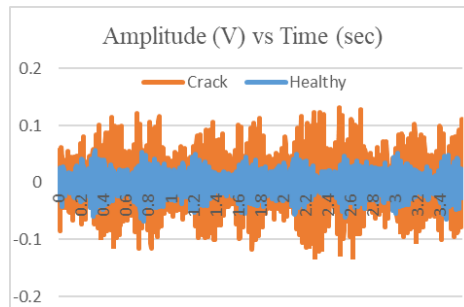


Fig. 2 Time-domain vibration signals of gear in healthy and crack condition

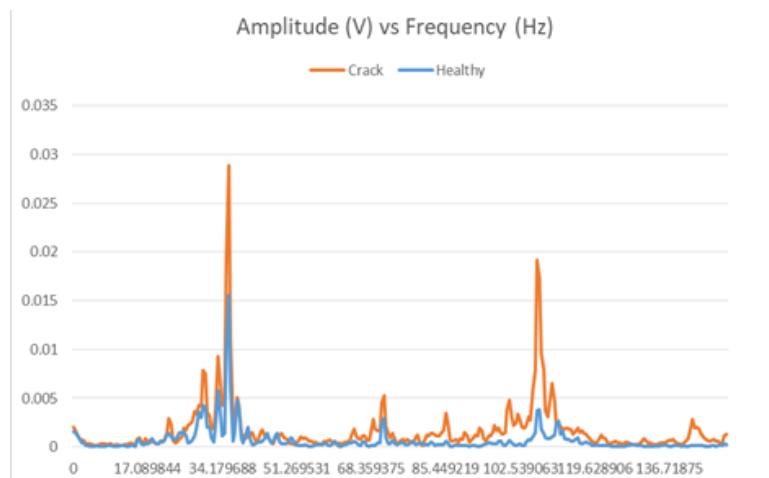


Fig. 3 Frequency-domain vibration signals of gear in healthy and crack condition

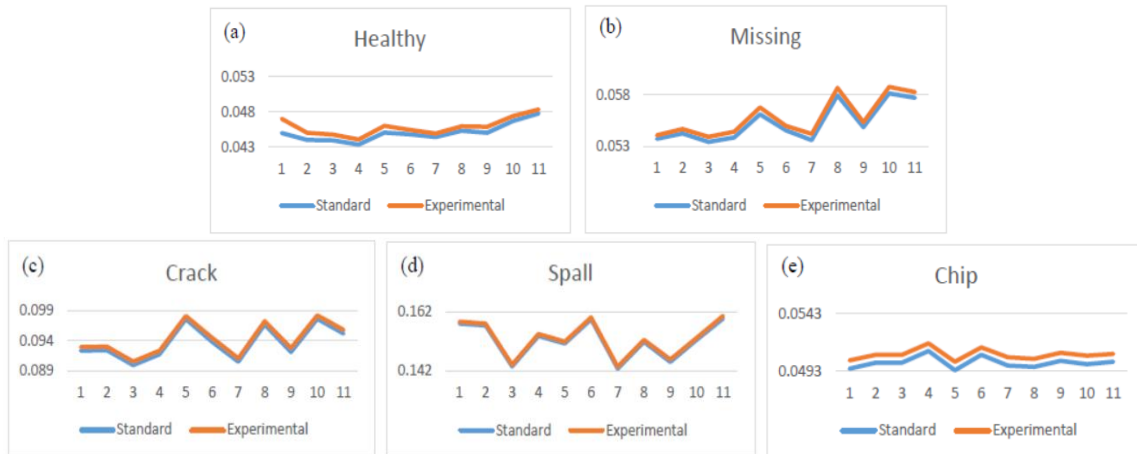


Fig. 4 RMS Feature Vector under varied conditions; (a) Healthy, (b) Missing teeth, (c) Crack, (d) Spall and (e) Chip

4.2 Dataset for extraction of feature vectors

An open-source dataset (Figshare Dataset *et al.* 2018) of gear vibration data for different fault conditions is used to extract feature vectors using the developed architecture. 11 samples are taken from the dataset for healthy, missing, crack, spall and chip conditions. Data such as frequency sampling rate, shaft frequency, number of gear teeth and gear mesh frequency are not available in the dataset. Assuming a sample rate, the frequency spectrum of the raw vibration is generated for each condition using the FFT algorithm. The range of sideband frequencies about the gear mesh frequency and its harmonics are determined from the FFT plot for healthy and crack conditions. The frequency corresponding to the first peak in the spectrum (i.e., shaft frequency) is also determined and compared with the difference between the sideband and gear mesh frequencies of vibration signals in time-domain and frequency domain are illustrated in Figs. 2-3, respectively. An approximate assumption is made for the values of shaft frequency and gear mesh frequency by comparing the ranges for the samples.

Approximate Assumptions: Frequency Sampling Rate= 18000 Hz, Shaft Frequency= 40 Hz, Number of Gear Teeth= 16, Gear Mesh Frequency= 640 Hz

5. Results and discussions

5.1 Feature vectors derived from the fault diagnosis architecture

The feature vectors are determined by applying the gear fault diagnosis architecture on the vibration data for healthy, missing, crack, spall and chip conditions experimentally and, are compared with using own code in MATLAB which are named as standard results. The y-coordinate is the magnitude of feature vector and the x-coordinate is the sample number. The line denotes the variation of feature vector with the sample points which are explained in all Figs. 4-10. Referring to Fig. 4, for the RMS feature vector, the value for all fault conditions is greater than the value for healthy condition. Due to faults, the amplitude and energy content of the vibration

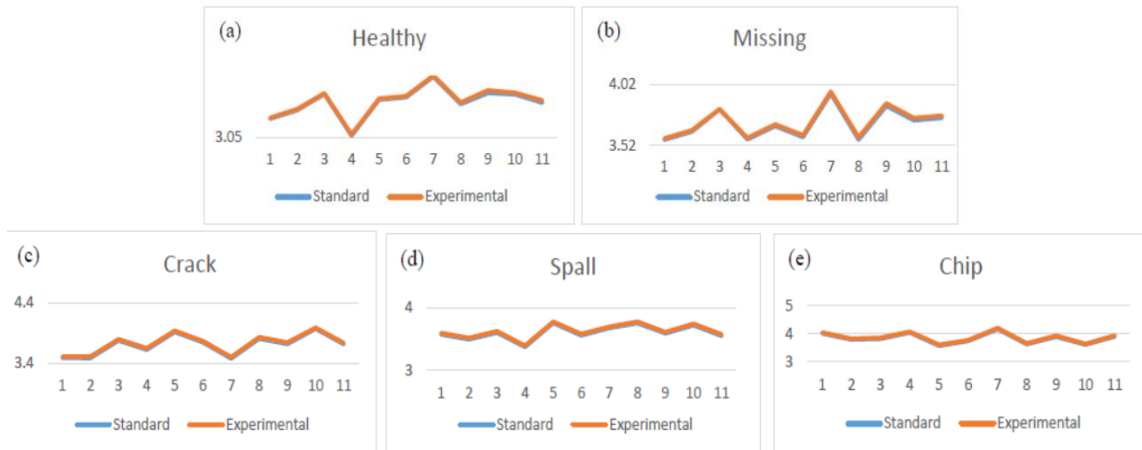


Fig. 5 Kurtosis Feature Vector under varied conditions; (a) Healthy, (b) Missing teeth, (c) Crack, (d) Spall and (e) Chip



Fig. 6 Crest Factor Feature Vector under varied conditions; (a) Healthy, (b) Missing teeth, (c) Crack, (d) Spall and (e) Chip

increases and this is evident from the experimental and standard results. Spall (Progressive Wear) condition has the highest levels of vibration, so the RMS feature vector is maximum for the Spall condition.

As shown in Fig. 5, the kurtosis feature vector, the value for all fault conditions is greater than the value for healthy condition. Due to faults, there is a higher presence of peaks in the vibration spectrum and these shows in the experimental and the standard results. Chip (Partially Broken Tooth) condition leads to the occurrence of greater number of peaks over a sampling rate, so the Kurtosis feature vector is maximum for the chip condition.

For the Crest Factor feature vector as illustrated in Fig. 6, the value for missing, crack and chip conditions is greater than the value for healthy condition. For spall condition, the value is less than the value for healthy condition. Due to all faults except spall, the maximum vibration amplitude and the vibration RMS increase at nearly the same proportion compared to the values at Healthy

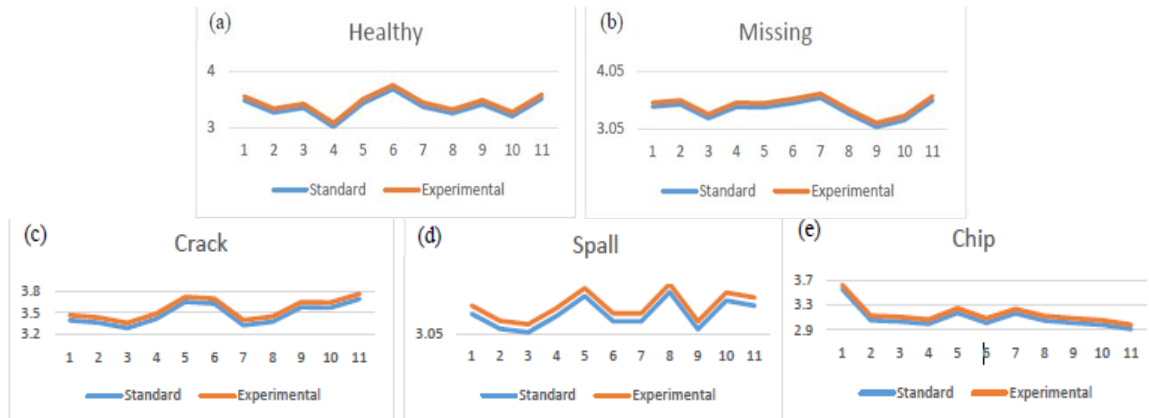


Fig. 7 FM4 Feature Vector under varied conditions; (a) Healthy, (b) Missing teeth, (c) Crack, (d) Spall and (e) Chip

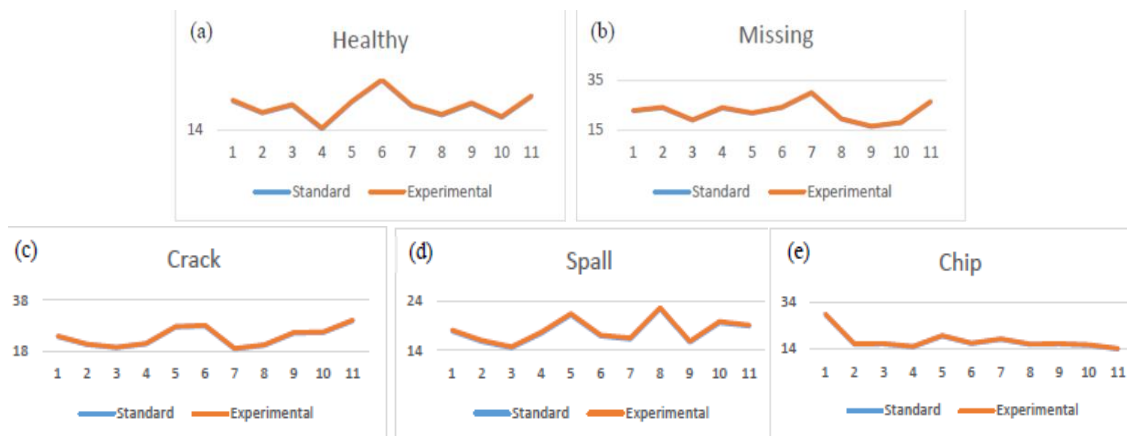


Fig. 8 M6A Feature Vector under varied conditions; (a) Healthy, (b) Missing teeth, (c) Crack, (d) Spall and (e) Chip

condition. For Spall condition, the vibration RMS increases at a greater proportion than the maximum vibration amplitude compared to the values at Healthy condition. Chip condition gives rise to the highest proportional increase in the vibration amplitude compared to the vibration RMS, so the Crest Factor feature vector is maximum for chip condition.

For the FM4, M6A and M8A feature vectors as shown in Figs. 7-9, the values for missing and crack conditions are greater than the values for healthy condition. For spall and chip conditions, the values are less than the values for Healthy condition. For Spall and Chip conditions, due to removal of the first order sidebands in the differential signals, the presence of peaks in the vibration spectrum is reduced compared to the healthy condition and this is evident in the experimental and the standard results. Crack condition leads to the occurrence of greater number of peaks over a sampling rate, so the FM4, M6A and M8A feature vectors are maximum for Crack condition.

For the energy ratio feature vector, the value for spall and chip conditions is greater than the value for healthy condition. For missing and crack conditions, the value is less than the value for

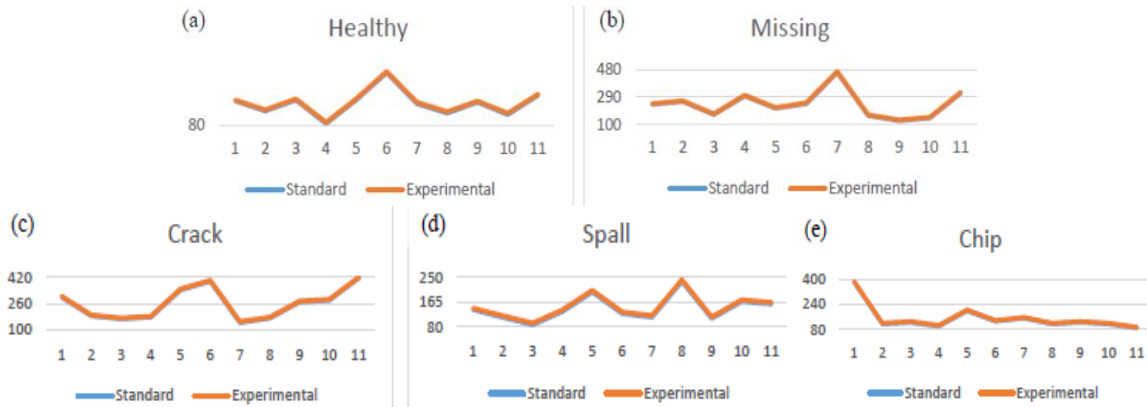


Fig. 9 M8A feature vectors under varied conditions; (a) Healthy, (b) Missing teeth, (c) Crack, (d) Spall and (e) Chip

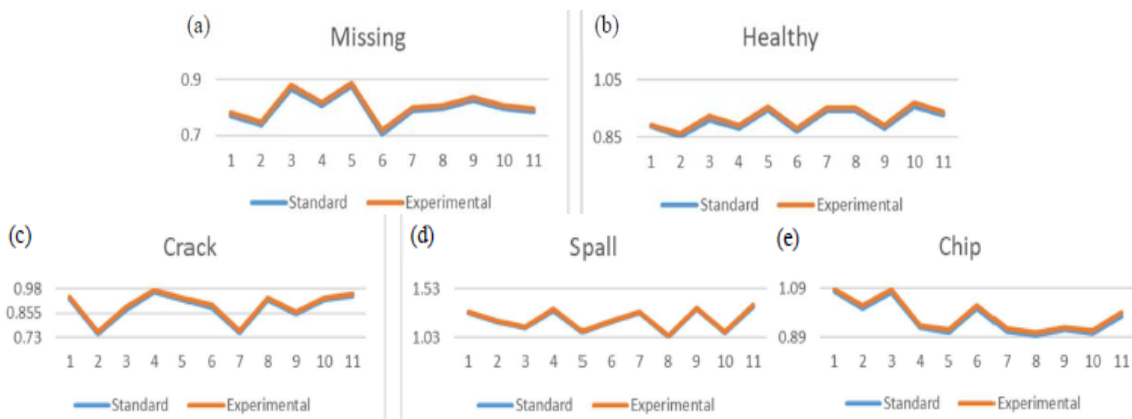


Fig. 10 Energy ratio feature vector under varied conditions; (a) Healthy, (b) Missing teeth, (c) Crack, (d) Spall and (e) Chip

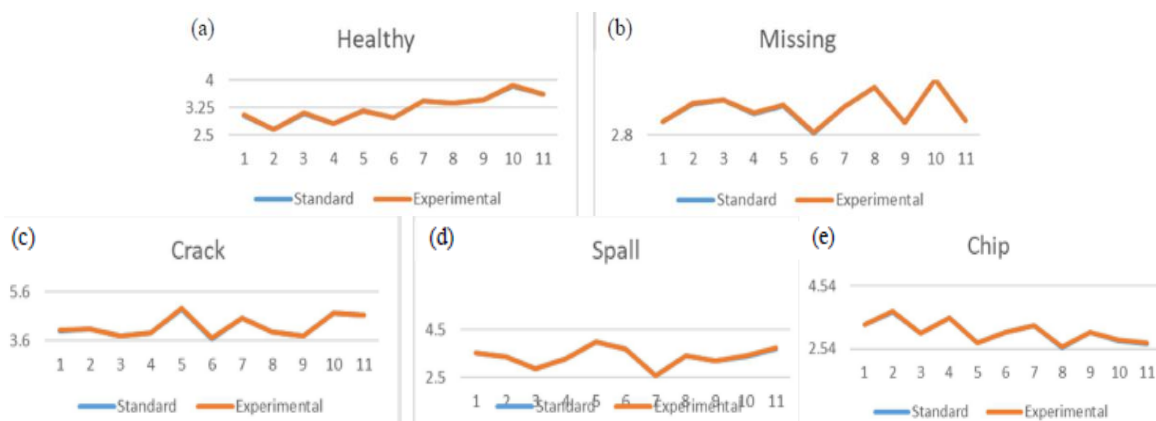


Fig. 11 NA4 feature vectors under varied conditions; (a) Healthy, (b) Missing teeth, (c) Crack, (d) Spall and (e) Chip

Table 1 Feature vectors for different gear faults

Fault condition	Appropriate feature vectors
Missing teeth	
Crack	FM4, M6A, M8A, NA4
Spall	RMS, Energy ratio
Chip	Kurtosis, Crest factor

healthy condition. For missing and crack conditions, the increase in energy content of the regular meshing components is comparatively higher than the increase in the energy content of the differential signal and this is evident in the experimental and the standard results. Spall condition leads to the occurrence of high energy content of the differential signal compared to the regular meshing components, so the Energy Ratio feature vector is maximum for Spall condition.

For the NA4 feature vector as shown in Fig. 11, the value for all fault conditions except chip is greater than the value for healthy condition. For chip condition, the value is less than the value for healthy condition. Due to all faults except chip, the energy content of the residual signal gradually decreases along the run ensemble and this decrease in the energy content is not balanced by the presence of peaks in the vibration spectrum. Crack condition has the highest gradual decrease in the energy content of the residual signal along the run ensemble, so the NA4 feature vector is maximum for Crack condition.

5.2 Observations in characteristics of feature vectors

For performance evaluation of the gear fault diagnosis architecture, the experimental results are compared with the standard results. From the plots as shown in Figs. 4-11, of the feature vectors it is observed that:

- The experimental results are almost similar to the standard results for RMS feature vector for the given fault conditions, the deviation being maximum for chip condition.
- The experimental results are almost similar to the standard results for Kurtosis feature vector for the given fault conditions.
- The experimental results are almost similar to the standard results for Crest Factor feature vector for the given fault conditions, the deviation being maximum for spall condition.
- The experimental results are almost similar to the standard results for FM4 feature vector for the given fault conditions, the deviation being maximum for spall condition.
- The experimental results are almost similar to the standard results for M6A feature vector for the given fault conditions.
- The experimental results are almost similar to the standard results for M8A feature vector for the given fault conditions.
- The experimental results are almost similar to the standard results for energy ratio feature vector for the given fault conditions, the deviation being maximum for missing and crack conditions.
- The experimental results are almost similar to the standard results for NA4 feature vector for the given fault conditions.

For each type of gear fault (Missing teeth, Crack, Spall, Chip), the feature vector with the maximum value for a fault condition is chosen as the appropriate feature vector to be studied for

identifying that particular gear fault from acquired raw vibration signals. The appropriate feature vectors for each fault are given in the Table 1.

6. Conclusions

The developed gear fault diagnosis architecture gives results that are comparable with results obtained from MATLAB. The pattern of the feature vectors is found to be similar for both cases for the given fault conditions and the physical significance of pattern of each feature vector is deduced. The appropriate feature vectors to be studied for Crack, Spall and Chip condition are determined.

The result dataset can be divided into training dataset and testing dataset in the ratio 80:20 which would be used for developing artificial intelligence based expert systems for gear fault diagnosis.

The feature vectors extracted using the developed algorithm can be further processed using data analysis techniques to determine the most suitable feature vector for each fault condition of the gear. This will help in the development of an advanced gear fault diagnosis system.

The developed gear fault diagnosis system can be further developed into an expert artificial intelligence system using algorithms like Support Vector Machine (SVM), Bayesian networks, and Artificial Neural Networks (ANN). The expert system can predict failure in the gear drive of the combat aircraft engines and deduce the type of failure.

References

- Abu-Mahfouz, I.A. (2005), "A comparative study of three artificial neural networks for the detection and classification of gear faults", *Int. J. General Syst.*, **34**(3), 261-277.
<https://doi.org/10.1080/03081070500065726>.
- Bansal, S., Sahoo, S., Tiwari, R., and Bordoloi, D.J. (2013), "Multiclass fault diagnosis in gears using support vector machine algorithms based on frequency domain data", *Measurement*, **46**(9), 3469-3481.
<https://doi.org/10.1016/j.measurement.2013.05.015>.
- Bartelmus, W., and Zimroz, R. (2009), "Vibration condition monitoring of planetary gearbox under varying external load", *Mech. Syst. Signal Pr.*, **23**(1), 246–257. <https://doi.org/10.1016/j.ymsp.2008.03.016>.
- Bartelmus, W., and Zimroz, R. (2009), "A new feature for monitoring the condition of gearboxes in non-stationary operating conditions", *Mech. Syst. Signal Pr.*, **23**(1), 1528-1534.
<https://doi.org/10.1016/j.ymsp.2009.01.014>.
- Bechhoefer, E., Qu, Y., Zhu, J., and He D. (2013), "Signal processing techniques to improve an acoustic emission sensor," *Annual Conference of the Prognostics and Health Management Society*, **4**, 1-8.
<https://doi.org/10.36001/phmconf.2013.v5i1.2174>.
- CBM Connect (2020), GMF Calculation and Gearbox Problems Detection;
www.cbmconnect.com/gmfcalculationandgearboxproblemsdetection/.
- Chaari, F., Fakhfakh, T. and Haddar, M. (2006), "Dynamic Analysis of a planetary gear failure caused by tooth pitting and cracking", *J. Fail. Anal. Prev.*, **6** (2),73-78. <https://doi.org/10.1361/154770206X99343>.
- Chen, H., Sun, Y., Shi, Z. and Lin, J. (2016), "Intelligent analysis method of gear faults based on FRWT and SVM", *Shock Vib.*, **2016**, 1582738. <https://doi.org/10.1155/2016/1582738>.
- Cheng, G., Cheng, Y. and Shen, L. *et al.* (2013), "Gear fault identification based on Hilbert-Huang transform and SOM neural network", *Measurement*, **46** (3), 1137-1146.
<https://doi.org/10.1016/j.measurement.2012.10.026>.

- Chen, D., Wang, and W.J. (2002), "Classification of wavelet map patterns using multi-layer neural networks for gear fault detection", *Mech. Syst. Signal Pr.*, **16**(4), 695-704. <https://doi.org/10.1006/mssp.2002.1488>.
- Chen X, Hong J, Wang Y, and Ma Y (2021), "Fatigue failure analysis of the central-driven bevel gear in a turboshaft engine arising from multi-source excitation", *Eng. Fail. Anal.*, **119**, 104811. <https://doi.org/10.1016/j.engfailanal.2020.104811>.
- Cirrincione, G., Kumar,R.R, Mohammadi, A., Kia, S.H., Barbiero, P. and Ferrett, J. (2020), "Shallow versus deep neural networks in gear fault diagnosis", *IEEE T. Energy Convers.*, **35**(3), 1338-1347. <https://doi.org/10.1109/TEC.2020.2978155>.
- Čular I, Vučković K, Galić I, and Žeželj D (2023), "Computational model for bending fatigue life and failure location prediction of surface-hardened running gears", *Int. J. Fatigue*, **166**, 107300. <https://doi.org/10.1016/j.ijfatigue.2022.107300>.
- Decker, H.J. (2002), "Crack detection for aerospace quality spur gears," NASA TM-2002-211492, ARL-TR-2682, NASA and the US Army Research Laboratory.
- Decker, H.J. and Lewicki, D.G. (2003), "Spiral bevel pinion crack detection in a helicopter gearbox, Proceedings of the American Helicopter Society", 59th Annual Forum, 1222-1232, Phoenix, Arizona.
- Dempsey, P.J. and Zakrajsek, J.J. (2001), "Minimizing load effects on NA4 gear vibration diagnostic parameter", *Proceedings of the 55th Meeting sponsored by the Society for Machine Failure Prevention Technology*, Virginia Beach, Virginia, April.
- Fernandez, A. (2022), Frequencies of a gear assembly; power-mi.com/content/frequencies-gear-assembly.
- Feng, Z.P., Liang, M., Zhang, Y. and Zhang, Y. (2012), "Fault diagnosis for wind turbine planetary gearboxes via demodulation analysis based on ensemble empirical mode decomposition and energy separation", *Renew. Energy*, **47**, 112-126. <https://doi.org/10.1016/j.renene.2012.04.019>.
- Figshare Dataset (2018), Gear Fault Data; figshare.com/articles/dataset/Gear_Fault_Data/6127874/1.
- GearConditionMetrics (2019), Standard Metrics for Gear Condition Monitoring; www.mathworks.com/help/predmaint/ref/gearconditionmetrics.html.
- Heydari, A. (2021), "The damped vibration of the annular and rectangular graded beams in the presence of the attached lumped mass", *Adv. Comput. Des.*, **6**(4), 329-338. <https://doi.org/10.12989/acd.2021.6.4.329>.
- Hines, J.A., Muench, D.S. and Keller, J.A. (2005), "Effects of time-synchronous averaging implementations on HUMS features for UH-60A planetary carrier cracking", *Annual Forum Proceedings-American Helicopter Society*, Grapevine, Texas, U.S.A., June.
- Huangfu, Y., Zhao, Z., Ma, H., Han, H. and Chen, K. (2020), "Effects of tooth modifications on the dynamic characteristics of thin-rimmed gears under surface wear", *Mech. Mach. Theory*, **150**, 103870. <https://doi.org/10.1016/j.mechmachtheory.2020.103870>.
- James, C.L. and Limmer, J.D. (2000), "Model-based condition index for tracking gear wear and fatigue damage", *Wear*, **241**(1), 26-32. [https://doi.org/10.1016/S0043-1648\(00\)00356-2](https://doi.org/10.1016/S0043-1648(00)00356-2).
- Jiang, Y.H., Tang, B.P. and Qin, Y. *et al.* (2011), "Feature extraction method of wind turbine based on adaptive Morlet wavelet and SVD", *Renewable Energy*, **36**(8), 2146-2153. <https://doi.org/10.1016/j.renene.2011.01.009>.
- Jing, L., Zhao, M., Li, P. and Xu, X. (2017), "A convolutional neural network-based feature learning and fault diagnosis method for the condition monitoring of gearbox", *Measurement*, **111**, 1-10. <https://doi.org/10.1016/j.measurement.2017.07.017>.
- Keller, J.A. and Grabill, P. (2003), "Vibration monitoring of UH-60A main transmission planetary carrier fault", *American Helicopter Society 59th Annual Forum*, Phoenix, Arizona, U.S.A., May.
- Li, W., Zhang, L. and Xu, Y. (2012), "Gearbox pitting detection using linear discriminant analysis and distance preserving self-organizing map", *IEEE International Instrumentation and Measurement Technology Conference Proceedings*, 2225-2229. <https://doi.org/10.1109/I2MTC.2012.6229667>.
- Liu, W.Y., Zhang, W.H., Han, J.G. and Wang, G.F. (2012), "A new wind turbine fault diagnosis method based on the local mean decomposition", *Renewable Energy*, **48**, 411-415. <https://doi.org/10.1016/j.renene.2012.05.018>.
- Liu, X., Yang, Y. and Zhang, J. (2018), "Resultant vibration signal model-based fault diagnosis of a single-stage planetary gear train with an incipient tooth crack on the sun gear", *Renewable Energy*, **122**, 65-79.

- <https://doi.org/10.1016/j.renene.2018.01.072>.
- Luo, Y., Cui, L., Zhang, J. and Ma, J. (2021), "Vibration mechanism and improved phenomenological model of planetary gearbox with broken sun gear fault", *Measurement*, **178**, 109356. <https://doi.org/10.1016/j.measurement.2021.109356>.
- Ma, H., Pang, X., Feng, R., Song, R. and Wen, B. (2015), "Fault features analysis of cracked gear considering the effects of the extended tooth contact", *Eng. Fail. Anal.*, **48**, 105-120. <https://doi.org/10.1016/j.engfailanal.2014.11.018>.
- Machinery Lubrication (2022), How to Analyze Gear Failures: Noria corporation, Tusla, U.S.A. www.machinerylubrication.com/Read/150/.
- Mark, W.D., Lee, and Patrick, H.R. and Coker, J.D. (2010), "A simple frequency-domain algorithm for early detection of damaged gear teeth", *Mech. Syst. Signal Pr.*, **24**, 2807-2823. <https://doi.org/10.1016/j.ymsp.2010.04.004>.
- McFadden, P.D. (1991), "A technique for calculation the time domain averages of the vibration of the individual planet gears and the sun gear in an epicyclic gearbox", *J. Sound Vib.*, **144**(1), 163-172. [https://doi.org/10.1016/0022-460X\(91\)90739-7](https://doi.org/10.1016/0022-460X(91)90739-7).
- McFadden, P.D. and Howard, I.M. (1990), "The detection of seeded faults in an epicyclic gearbox by signal averaging of the vibration", Technical Report, Propulsion Report 183, Aeronautical Research Laboratory, Melbourne, Australia.
- McNames, J. (2001), "Fourier series analysis of epicyclic gearbox vibration", *J. Vib. Acoust.*, **124**, 150-153. <https://doi.org/10.1115/1.1403735>.
- Prabhu R, and Devaraju A. (2021), "Failure analysis and restructuring model of transfer feeder gear box in thermal powerplant", *Mater. Today Proc.*, **39**, 633-638. <https://doi.org/10.1016/j.matpr.2020.08.808>.
- Qiang, Z., Jieying, G., Junming, L., Ying, T. and Shilei, Z. (2020), "Gearbox fault diagnosis using data fusion based on self-organizing map neural network", *Int. J. Distrib. Sens. N.*, **16**(5), 1-11. <https://doi.org/10.1177/1550147720923476>.
- Rolls-Royce (2015), *The Jet Engine*, 5th edition, Wiley, New York, U.S.A.
- Sanz, J., Perera, and Huerta, R.C. (2012), "Gear dynamics monitoring using discrete wavelet transformation and multi-layer perceptron neural networks", *Appl. Soft Comput.*, **12**(9), 2867-2878. <https://doi.org/10.1016/j.asoc.2012.04.003>.
- Saravanan, N., Siddabattuni, V.N.S.K. and Ramachandran, K.I. (2010), "Fault diagnosis of spur bevel gear box using artificial neural network (ANN) and proximal support vector machine (PSVM)", *Appl. Soft Comput.*, **10**(1), 344-360. <https://doi.org/10.1016/j.asoc.2009.08.006>.
- Saxena, A., Wu, B.Q. and Vachtsevanos, G. (2005), "A methodology for analyzing vibration data from planetary gear systems using complex Morlet wavelets", *Proceedings of the 2005, American Control Conference*, 4730-4735, Portland, Oregon, U.S.A., June. <https://doi.org/10.1109/ACC.2005.1470743>.
- Schön, P.P. (2005), "Unconditionally convergent time domain adaptive and time-frequency techniques for epicyclic gearbox vibration", Mechanical and Aeronautical Engineering, Master Thesis, University of Pretoria, Pretoria, South Africa.
- Shen, C.H., Wen, J., Arunyanart, P. and Choy, F.K. (2011), "Vibration signature analysis and parameter extractions on damages in gears and rolling element bearings", *ISRN Mech. Eng.*, **2011**, 402928. <https://doi.org/10.5402/2011/40292>.
- Singleton, K. (2006), "Case Study-Analysis of two-stage planetary gearbox vibration", KSC Consulting LLC, Case Study.
- Smidt, M.R. (2010), "Internal vibration monitoring of a planetary gearbox", Master Thesis, University of Pretoria, Pretoria, South Africa.
- Sparis, G.P. and Vachtsevanos, N.D (2022), "Automatic diagnostic feature generation via the fast fourier transform", Technical Report.
- Sunder, S.T. and Hemalatha, S. (2021), "Experimental analysis of mechanical vibration in 225 kW wind turbine gear box", *Mater. Today Pr.*, **46**, 3292-3296. <https://doi.org/10.1016/j.matpr.2020.11.461>.
- Večeř, P., Kriedl M. and Šmíd R. (2005), "Condition Indicators for gearbox condition monitoring systems", *Acta Polytechnica*, **45**(6), 35-43.

- Wang, W. (2001), "Early detection of gear tooth cracking using the resonance demodulation technique", *Mech. Syst. Signal Pr.*, **15**, 887-903. <https://doi.org/10.1006/mssp.2001.1416>.
- Wang, X. and Makis, V. (2009), "Autoregressive model-based gear shaft fault diagnosis using the Kolmogorov-Smirnov test," *J. Sound Vib.*, **327**(3-5),413-423. <https://doi.org/10.1016/j.jsv.2009.07.004>.
- Wu, B.Q., Saxena A, and Patrick R, Vachtsevanos, G. (2005), "Vibration monitoring for fault diagnosis of helicopter planetary gears", *IFAC Proceedings Volumes*, **38**(1), 755-60. <https://doi.org/10.3182/20050703-6-CZ-1902.00127>.
- Wu, S., Zuo, M.J. and Parey, A. (2008), "Simulation of spur gear dynamics and estimation of fault growth", *J. Sound Vib.*, **317**, 608-624. <https://doi.org/10.1016/j.jsv.2008.03.038>.
- Xing, Z., Qu, J., Chai, Y., Tang, Q. and Zhou, Y. (2017), "Gear fault diagnosis under variable conditions with intrinsic time-scale decomposition-singular value decomposition and support vector machine", *J. Mech. Sci. Technol.*, **31**(2), 545-553. <https://doi.org/10.1007/s12206-017-0107-3>.
- Yang, X., Ding, K. and He, G. (2019), "Phenomenon-model-based AM-FM vibration mechanism of faulty spur gear", *Mech. Syst. Signal Pr.*, **134**, 106366. <https://doi.org/10.1016/j.ymsp.2019.106366>.
- Yip, L. (2011), "Analysis and modelling of planetary gearbox vibration data for early fault detection", Master Thesis, University of Toronto, Toronto, Canada 2011. <https://hdl.handle.net/1807/31653>.
- Yu, J. (2011), "Early fault detection for gear shaft and planetary gear based on wavelet and hidden Markov modeling", Doctoral Thesis, University of Toronto, Toronto, Canada.
- Li, Y.X., Jiao, S.B., Geng, B., Zhang, Q. and Zhang, Y.M. (2022), "A comparative study of four nonlinear dynamic methods and their applications in classification of ship-radiated noise", *J. Defense Technol.*, **18**(2), 183-193. <https://doi.org/10.1016/j.dt.2020.11.011>.
- Li, Y.X., Jiao, S.B. and Gao, X. (2021), "A novel signal feature extraction technology based on empirical wavelet transform and reverse dispersion entropy", *J. Defense Technol.*, **17**(5), 1625-1635. <https://doi.org/10.1016/j.dt.2020.09.001>.
- Zakrajsek, J.J. and Lewicki, D.G. (1996), "Detecting gear tooth fatigue cracks in advance of complete fracture", NASA TM-107145, ARL TR-970, NASA and the US Army Aviation Systems Command, April.
- Zakrajsek, J.J., Townsend, D.P. and Decker, H.J. (1993), "An analysis of gear fault detection methods as applied to pitting fatigue failure data", NASA TM-105950, AVSCOM TR-92-C-035, NASA and the US Army Aviation Systems Command, January.
- Zhang, X.H., Kang J.S., Zhao, J.S. and Cao, D.C. (2013), "Features for fault diagnosis and prognosis of gearbox", *Chem. Eng. Transact.*, **33**, 1027-1032.